Markov transition probability-based network from time series for characterizing experimental two-phase flow*

Gao Zhong-Ke(高忠科), Hu Li-Dan(胡沥丹), and Jin Ning-De (金宁德)†

School of Electrical Engineering and Automation, Tianjin University, Tianjin 300072, *China*

(Received 20 October 2012; revised manuscript received 14 November 2012)

We generate a directed weighted complex network by a method based on Markov transition probability to represent an experimental two-phase flow. We first systematically carry out gas–liquid two-phase flow experiments for measuring the time series of flow signals. Then we construct directed weighted complex networks from various time series in terms of a network generation method based on Markov transition probability. We find that the generated network inherits the main features of the time series in the network structure. In particular, the networks from time series with different dynamics exhibit distinct topological properties. Finally, we construct two-phase flow directed weighted networks from experimental signals and associate the dynamic behavior of gas–liquid two-phase flow with the topological statistics of the generated networks. The results suggest that the topological statistics of two-phase flow networks allow quantitative characterization of the dynamic flow behavior in the transitions among different gas–liquid flow patterns.

Keywords: complex network, time series analysis, chaotic dynamics, two-phase flow pattern

PACS: 05.45.Tp, 05.45.−a **DOI:** 10.1088/1674-1056/22/5/050507

1. Introduction

Gas–liquid two-phase flow exists widely in lubrication, nuclear reactor cooling, and well bores. In two-phase flow systems, e.g., gas–water two-phase flow, the flow pattern is defined by the temporal and spatial variation of the interfacial configuration of the two phases. The research interests in the characterization of flow patterns lie in the fact that different flow patterns have distinct hydrodynamic properties. Characterizing the dynamic behavior of gas–liquid flow patterns from experimental measurements has been an outstanding interdisciplinary problem in the fields of nonlinear time-series analysis and fluid dynamics. Vertical upward gas–water two-phase flow exhibits an unsteady and complex flow structure due to the existence of fluid turbulence, the local relative movements between gas and water phase, and the phase interfacial interaction. In addition, theoretical analyses have limitations as applied to uncover the nonlinear dynamics leading to the formation of different gas–liquid flow patterns. In this regard, developing a reliable method to effectively uncover the dynamic behavior underlying various gas–liquid flow patterns would be particularly useful.

Complex network theory has undergone excellent development in the last decade and has contributed significantly to our understanding of complex systems.[1–12] Complex networks can characterize many types of complex systems that contain a mass of entities interacting with each other in a complex manner. The investigation of complex systems in the framework of the complex network theory has attracted considerable attention as an interdisciplinary subject.[13–24] Recently, complex network theory has been introduced into the study of time series analysis, and complex network analysis of time series has attracted much attention from various research fields on account of its considerable importance.[25–45] Different approaches for mapping a time series into a complex network have been proposed, such as the approaches based on the concept of a quasi-periodic cycle,[25,26] correlations,[27] visibility,[28–33] transition probabilities,[34–36] recurrence analysis (phase-space reconstruction),[37–44] etc. Complex network analysis of time series has been successfully applied in many research fields, such as network topology estimation,[46–48] climate systems,[49–51] financial systems,[52,53] human gait,[54] human brain,[55] human ventricular fibrillation,[56] gene systems,[57] two-phase flow systems,[58–61] grain property networks,[62] friction networks in nucleation processes,[63] etc. Note that for an unweighted and undirected network, all the links are considered equivalent, but it is important to realize that different nodes and links make different contributions to the overall performance of a complex network,[64,65] i.e., many complex networks are directed and weighted such that the interaction between two nodes can be characterized not only by the existence of a link but also a link with a direction and a varying weight assigned to it. The investigation in the directed and weighted network aspect may provide deep insights for understanding the underlying mechanism of complex systems.

*Project supported by the National Natural Science Foundation of China (Grant Nos. 61104148, 41174109, and 50974095), the National Science and Technology Major Project of the Ministry of Science and Technology of China (Grant No. 2011ZX05020-006), and the Specialized Research Fund for the Doctoral Program of Higher Education of China (Grant No. 20110032120088).

†Corresponding author. E-mail: ndjin@tju.edu.cn

© 2013 Chinese Physical Society and IOP Publishing Ltd

By transforming a time series into a directed and weighted complex network, it is possible to study the dynamical properties of time series by using the mathematical knowledge from weighted network science. In this regard, bridging time series analysis and directed weighted complex network can be an appealing approach for experimental data analysis and flow pattern characterization.

In this paper, we use a Markov transition probability-based network to characterize the dynamic behavior of experimental gas–liquid flow patterns. First, we systematically carry out gas–liquid two-phase flow experiments to measure the flow signals corresponding to five different flow patterns. Then we use a network generation method based on the Markov transition probability to construct the directed weighted complex networks from different types of time series. Through investigating the network topological indices, we find that the generated directed weighted network inherits the main features of the time series in the network structure. In particular, the networks from time series with different dynamics exhibit distinct topological properties. Finally, we generate two-phase flow directed weighted networks from experimental signals and associate the dynamic behavior of gas–liquid two-phase flow with the topological statistics of the constructed networks. The results indicate that the topological statistics of the two-phase flow directed weighted networks, such as the weighted clustering coefficient, are very sensitive to the transitions among different flow patterns, and allow characterizing the nonlinear dynamics underlying different gas–liquid flow patterns. These interesting and significant findings suggest that the Markov transition probability-based network can potentially be a powerful tool for characterizing the dynamic behavior of gas–liquid two-phase flow patterns.

2. Experiments and data acquisition

The vertical upward gas–liquid two-phase flow experiment in a 125-mm diameter pipe was carried out in the two-phase flow laboratory of Tianjin University. The experimental media, i.e., the two phases are air and tap water. The experimental system includes a vertical plexiglass pipe, a vertical multi-electrode array conductance sensor, a digital high-speed dynamic video camera recorder, an exciting-signal generating circuit, a data-acquisition card PXI 4472 which is the product of National Instruments, a signal modulating module that consists of a differential amplifier sub-module, a sensitive demodulation sub-module, a low-pass filter sub-module, and a signal preprocessing module realized by LABVIEW 7.1 to display and store data in real-time. We implemented the vertical upward gas–water two-phase flow experiments by initially injecting both air and water flows into a 125-mm diameter pipe. We fixed the water flow rate and then gradually increased the air flow rate. In the experiment, the water flow rate was in the range from 0.02 m/s to 0.27 m/s and the air flow rate was between 0.0045 m/s and 2.94 m/s. We used the exciting-signal generating circuit to generate and input a 20-kHz sinusoidal voltage signal of amplitude 1.4 V to excite the air–water concurrent flow. For one fixed water flow rate, each time the air flow rate and water flow rate reach a pre-defined ratio, we collected conductance signals from the vertical multi-electrode array conductance sensor, and the flow pattern could be visualized and defined by using a digital high-speed dynamic video camera recorder. The sampling frequency was 400 Hz and the measuring time for one measurement was 60 s. Note that the conductance signals from the vertical multi-electrode array conductance sensor are very sensitive to the transitions of flow patterns and allow conducting complex network analysis to investigate the dynamic flow behavior. In our experiment, with the increase of the gas flow rate five types of vertical upward gas–liquid flow patterns gradually appeared, i.e., bubble flow, bubble-slug transitional flow, slug flow, slug–churn transitional flow, and churn flow, as shown in Fig. 1. Figure 2 shows the conductance signals from the vertical multi-electrode array conductance sensor for five gas–liquid flow patterns displayed in Fig. 1, where U_{sg} and U_{sw} represent the gas superficial velocity and the water superficial velocity, respectively.

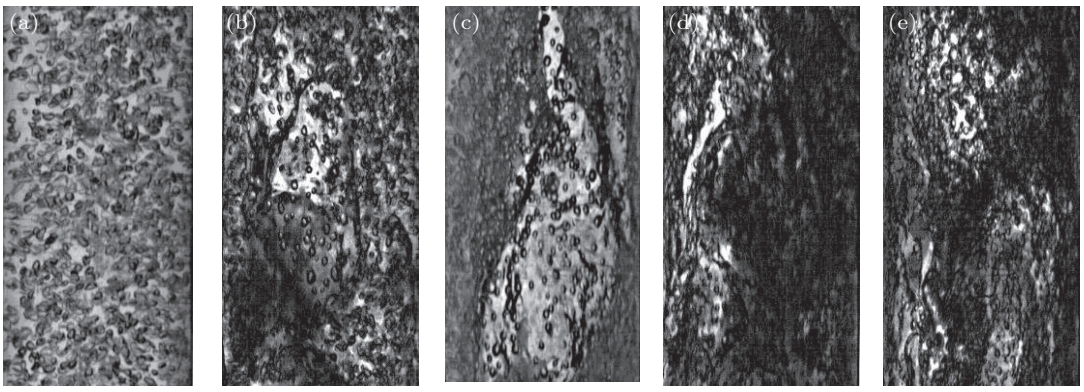


Fig. 1. The five vertical upward gas–water two-phase flow patterns recorded by using a high speed video camera recorder (VCR) system (the resolution is 640 × 480 and the frame rate is 200 frame/s): (a) bubble flow, (b) bubble-slug transitional flow, (c) slug flow, (d) slug-churn transitional flow, and (e) churn flow.

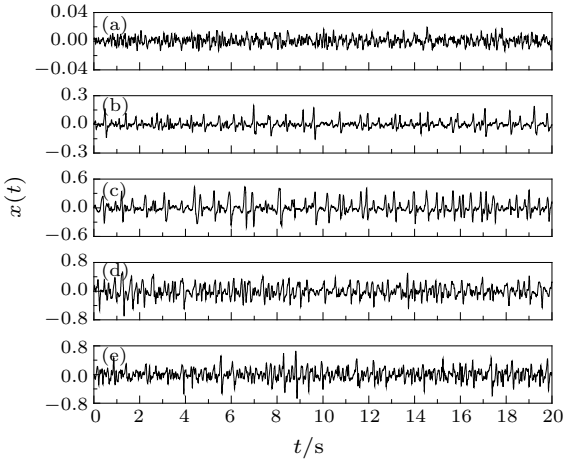


Fig. 2. The conductance fluctuating signals in five gas–water flow patterns: (a) bubble flow $U_{sw} = 0.18$ m/s and $U_{sg} = 0.01$ m/s, (b) bubble-slug transitional flow $U_{sw} = 0.18$ m/s and $U_{sg} = 0.04$ m/s, (c) slug flow $U_{sw} = 0.18$ m/s and $U_{sg} = 0.12$ m/s, (d) slug-churn transitional flow $U_{sw} = 0.18$ m/s and $U_{sg} = 0.35$ m/s, and (e) churn flow $U_{sw} = 0.18$ m/s and $U_{sg} = 0.61$ m/s.

3. Characterizing time series from different dynamic systems

A Markov chain is a mathematical system that undergoes transitions from one state to another, between a finite or countable number of possible states. The Markov chain is a discrete-time process that is memoryless in the sense that, given the past states and the present state, the future behavior (or the next state) depends only on the present state and not on the sequence of events that preceded it. Usually, a Markov chain can be described by a directed graph, in which the edges are labeled by the Markov probabilities of going from one state to the other states. According to the network generation method based on the Markov transition probability proposed in Refs. [35] and [36], we can create the network representations of a time series as follows: Given a time series $x(t)$, we identify its Q quantiles, which divide the range of signal values into Q intervals (q_i, $i = 1, 2, 3, ..., Q$) with equal probability. Each interval is represented by a node in the generated complex network, correspondingly, the generated network has Q nodes. Nodes i and j are connected if the value of $x(t)$ in interval q_i changes to that in interval q_j in one time step. A weight w_{ij} of an edge is the transition probability in a Markov model estimated from the time series. In particular, the weight w_{ij} for the edge from node i to node j is determined by the probability that a point in interval q_i is followed by a point in interval q_j. Repeated transitions between intervals lead to edges in the generated network with larger weights. In Fig. 3 we demonstrate the construction of a directed weighted complex network from a time series. As can be seen, the time series is divided into four intervals, i.e., q_1, q_2, q_3, and q_4. Consequently, the equivalent network of the time series has four nodes. Since the value of $x(t)$ in interval q_1 changes to that in interval q_2 in one time step, node 1 and node 2 are connected in the generated network. The number of times for the transitions from interval q_1 to all other intervals is 4 and the number of times for the transitions from interval q_1 to interval q_2 is 3. Consequently, the weight w_{12} for the edge from node 1 to node 2, i.e., transition probability from interval q_1 to interval q_2, is 3/4. Therefore, we can calculate the weights for all the edges of the generated complex network, i.e., obtaining the directed weighted network matrix. For more detail about the selection of Q quantiles refer to Refs. [35] and [36]. Using the above method, we generated networks from a periodic sinusoidal time series, a white noise time series, and a chaotic time series, respectively (as shown in Fig. 4). The chaotic time series are the data from the x component of the Lorenz system

$$\begin{cases} \dfrac{dx}{dt} = \sigma(y-x), \\ \dfrac{dy}{dt} = x(\rho - z) - y, \\ \dfrac{dz}{dt} = xy - \beta z, \end{cases} \tag{1}$$

where $\sigma = 16$, $\rho = 45.92$, and $\beta = 4$ as shown in Fig. 4(c), and the data from the x component of the Rössler system

$$\begin{cases} \dfrac{dx}{dt} = -y - z, \\ \dfrac{dy}{dt} = x + ay, \\ \dfrac{dz}{dt} = b + z(x-c), \end{cases} \tag{2}$$

where $a = 0.2$, $b = 0.2$, and $c = 5.7$ as shown in Fig. 4(d).

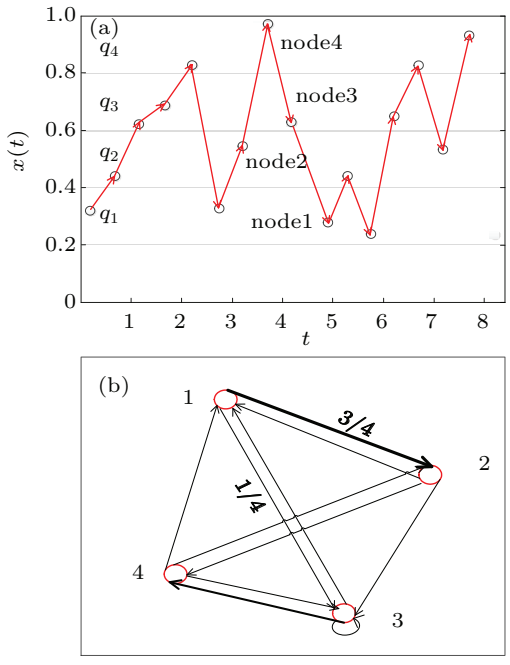


Fig. 3. (color online) The schematic diagram for the construction of a directed weighted complex network from a time series $x(t)$: (a) a time series $x(t)$, and (b) a directed weighted complex network from time series $x(t)$.

In Fig. 5, we show the topological structures of the directed weighted networks inferred from the four time series with different dynamics. It should be mentioned here that the network structures in Fig. 5 are drawn by using Ucinet and Netdraw software, and the algorithm used is the Kamada–Kawai spring embedding algorithm.[66]

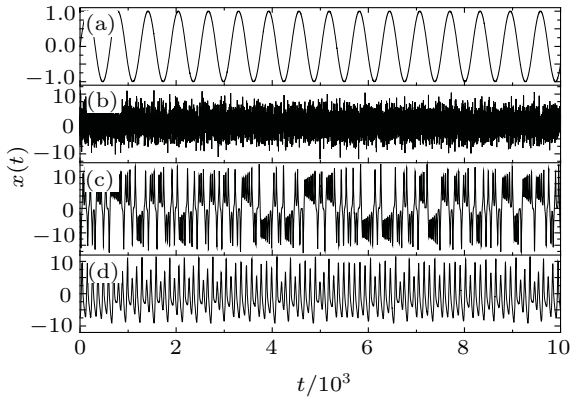


Fig. 4. Four time series with different dynamics for the construction of complex networks: (a) periodic sinusoidal time series, (b) Gaussian white noise time series, (c) chaotic time series from Lorenz system, and (d) chaotic time series from Rössler system.

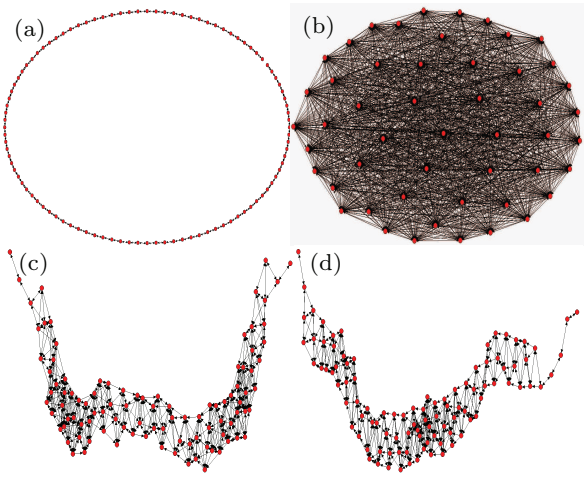


Fig. 5. (color online) Topological structures of complex networks generated from time series of length 10000 from (a) periodic sinusoidal system, (b) Gaussian white noise system, (c) chaotic Lorenz system, and (d) chaotic Rössler system. Structural skeletons of the various networks are drawn using Ucinet and Netdraw software.

As can be seen in Figs. 5(a) and 5(b), the generated network inherits the main properties of the time series in the network structure, and the networks from time series with different dynamics exhibit distinct topological properties. In particular, the network inferred from the periodic time series exhibits regular attributes, as shown in Fig. 5(a). In contrast, the network generated from the Gaussian white noise time series presents random properties in the sense that the nodes in the network are entangled with each other and the edges exist in an intersectional form, as can be seen in Fig. 5(b). The two complex networks from the chaotic time series both show a network configuration which is very similar to the chaotic attractor in phase space, i.e., the Lorenz and Rössler chaotic attractors, as shown in Figs. 5(c) and 5(d). Specifically, the nodes in a chaotic network congregate at different locations, leading to the existences of highly clustered regions and rather sparse regions. Distinguishing chaotic time series from random time series is a problem of continual interest. Now, we will demonstrate how to solve this problem in terms of the topological statistics of the constructed network, i.e., the weighted clustering coefficient. The weighted clustering coefficient of a node i measures how densely connected the neighborhood of the node i is,[35] and can be calculated as

$$C_i = \frac{\sum_{j,k} w_{ij} w_{jk} w_{ki}}{\sum_{j,k} w_{ij} w_{ki}}, \tag{3}$$

where w_{ij} is the weight for the edge from node i to node j. The weighted network clustering coefficient is the average of the weighted clustering coefficients for all nodes in the network, denoted as $\langle C \rangle$. We infer networks from the time series of length 60000 from the chaotic Lorenz system and white noise system, respectively, and then calculate the weighted network clustering coefficient $\langle C \rangle$ for the generated networks, as shown in Fig. 6. As can be seen, due to the existence of the unstable periodic orbits embedded in the chaotic attractor, the $\langle C \rangle$ of a chaotic network is obvious larger than that of a noisy network, which allows distinguishing chaotic time series from noisy time series. Furthermore, we investigate the anti-noise ability of the method by adding Gaussian white noise to the chaotic Lorenz time series to generate a time series whose signal-to-noise ratios is 20 dB. We find that, despite the intense influence of noise, the weighted clustering coefficient $\langle C \rangle$ is essentially larger than that of a network from a noisy time series, as shown in Fig. 6, indicating the robustness of the method.

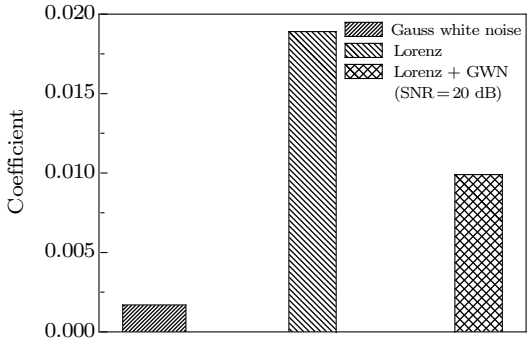


Fig. 6. Distributions of the weighted clustering coefficient of the networks generated from various time series of length 60000.

4. Characterizing flow behavior from experimental signals

We infer two-phase flow directed weighted networks from experimental signals of length 20000 by using the network generation method based on the Markov transition probability. The topological structures of the networks generated

from the signals of three typical flow patterns are shown in Fig. 7. As can be seen, the generated networks corresponding to different flow patterns exhibit different topological properties. Transforming a time series into a complex network, we can investigate the inherent structure and dynamical characteristics of a time series in terms of the knowledge from complex network theory. In particular, after representing an experimental signal through a corresponding directed weighted complex network, we can then study the dynamical behaviors of vertical upward gas–liquid flow patterns from complex network analysis, which is quantified via network topological statistics (e.g., the weighted network clustering coefficient $\langle C \rangle$). In order to characterize the dynamic behavior in the transitions among different flow patterns, we generate numbers of networks from experimental signals measured from different flow conditions. We then calculate the weighted network clustering coefficient $\langle C \rangle$ for each inferred network. Figure 8 displays the distributions of weighted clustering coefficient for 50 generated networks with the change of gas superficial velocity. We can see that the weighted clustering coefficient $\langle C \rangle$ for bubble flow is a small value, and this topological statistic will increase in the transition from bubble flow to slug flow. With a further increase of the gas superficial velocity, $\langle C \rangle$ decreases as the flow pattern evolves from slug flow to churn flow.

Vertical upward gas–liquid bubble flow occurs at low gas flow rates where the gas phase exists in the form of discrete gas bubbles and the small bubbles are approximately uniformly distributed in water continuous phase. Owing to the stochastic motions of a mass of small air bubbles, the dynamical behavior of bubble flow presents rather complicated features, corresponding to the small weighted network clustering coefficient. With the increase of the gas flow rate, numbers of small air bubbles begin to coalesce to form gas slugs of different sizes and slug flow gradually appears. Due to the quasi-periodic oscillation behavior associated with unstable periodic orbits between gas slug and liquid slug, the dynamical behavior of gas–liquid slug flow becomes relatively simple compared with that of bubble flow. Consequently, $\langle C \rangle$ will increase in the transition from bubble flow to slug flow, which agrees well with the results presented in Section 3. That is, due to the existence of unstable periodic orbits embedded in the chaotic attractor, the weighted clustering coefficient of the chaotic network is significantly larger than that of the noisy network, i.e., $\langle C \rangle$ will increase as the dynamics of the time series change from randomness to chaos. When the gas flow rate is very high, the churn flow that is composed of discrete gas phase and continuous liquid phase gradually appears. Due to the influence of highly turbulent kinetic energy, the oscillation behavior in churn flow is not so obvious as that in slug flow. Correspondingly, the dynamical behavior of churn flow becomes more complex than that of slug flow. Consequently, the value of the weighted clustering coefficient decreases as the flow pattern evolves from slug flow to churn flow, as shown in Fig. 8. Hence, the weighted clustering coefficient, which is very sensitive to the transitions among different flow patterns, allows effectively characterizing the distinct dynamic states of different gas–water flow patterns.

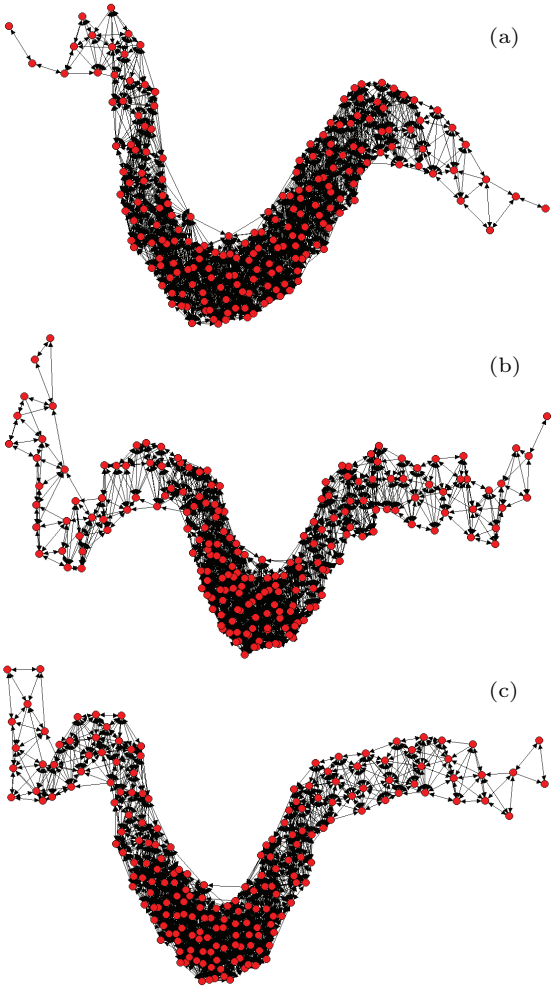


Fig. 7. (color online) The topological structures of the complex network generated from experimental signals of length 20000 from (a) bubble flow, (b) slug flow, and (c) churn flow. The topological structures of the networks are drawn using Ucinet and Netdraw software.

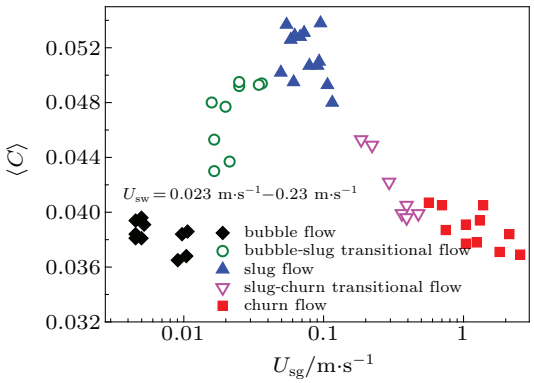


Fig. 8. (color online) The distributions of weighted clustering coefficient in semi-log scale for 50 generated networks with the increase of the gas superficial velocity.

5. Conclusions

Despite the tremendous body of established knowledge about fluid flows, our understanding of nonlinear dynamics leading to the formation of two-phase flow patterns is still quite limited. We first systematically carried out gas–liquid two-phase flow experiments for measuring signals corresponding to different flow patterns. Then, we generated the directed weighted complex networks from time series with different dynamics in terms of a network generation method based on the Markov transition probability. The results indicate that the constructed network can inherit the main features of the time series in the network structure. In addition, we demonstrated that the topological statistics of a generated network, such as the weighted clustering coefficient, allow distinguishing chaotic time series from noisy time series. Finally, we inferred two-phase flow directed weighted networks from experimental signals and found that the generated networks corresponding to different flow patterns exhibit different topological properties. In order to uncover the dynamic behavior in the transitions among different flow patterns, we constructed numbers of networks from experimental signals measured from different flow conditions and associate the dynamic behavior of gas–liquid flow patterns with the topological statistics of the generated networks. Furthermore, we demonstrated that the weighted clustering coefficient, which is very sensitive to the transitions among different flow patterns, allows quantitatively characterizing the dynamic flow behavior underlying different gas–liquid flow patterns.

References

[1] Albert R and Barabási A L 2002 *Rev. Mod. Phys.* **74** 47
[2] Wang W X, Wang B H, Hu B, Yan G and Ou Q 2005 *Phys. Rev. Lett.* **94** 188702
[3] Boccaletti S, Latora V, Moreno Y, Chavez M and Hwang D U 2006 *Phys. Rep.* **424** 175
[4] Huang L, Park K, Lai Y C, Yang L and Yang K Q 2006 *Phys. Rev. Lett.* **97** 164101
[5] Pan Z F, Li X and Wang X F 2006 *Phys. Rev. E* **73** 056109
[6] Li X G, Gao Z Y, Li K P and Zhao X M 2007 *Phys. Rev. E* **76** 016110
[7] Pei W D, Chen Z Q and Yuan Z Z 2008 *Chin. Phys. B* **17** 373
[8] Zhou J, Lu J A and Lu J H 2008 *Automatica* **44** 996
[9] Yu W, Cao J, Chen G, Lü J, Han J and Wei W 2009 *IEEE Trans. Systems, Man, Cybernetics-Part B* **39** 230
[10] Rong Z H, Wu Z X and Wang W X 2010 *Phys. Rev. E* **82** 047101
[11] Duan Z S and Chen G R 2012 *Chin. Phys. B* **21** 080506
[12] Lü L Y, Medo M, Ho Y C, Zhang Y C, Zhang Z K and Zhou T 2012 *Phys. Rep.* **519** 1
[13] Zheng D F, Hui P M, Trimper S and Zheng B 2005 *Physica A* **352** 659
[14] Jiang Z Q, Zhou W X, Xu B and Yuan W K 2007 *AIChE Journal* **53** 423
[15] Zhang H F, Small M, Fu X C and Wang B H 2009 *Chin. Phys. B* **18** 3639
[16] Guo J L 2010 *Chin. Phys. B* **19** 120503
[17] Lu X B, Wang X F and Fang J Q 2010 *Physica D* **239** 341
[18] Schneider C M, Moreira A A, Andrade Jr J S, Havlin S and Herrmann H J 2011 *Proc. Natl. Acad. Sci. USA* **108** 3838
[19] Zhang C, Shen H Z, Li F and Yang H Q 2012 *Acta Phys. Sin.* **61** 148902 (in Chinese)
[20] Wang D L, Yu Z G and Anh V 2012 *Chin. Phys. B* **21** 080504
[21] Yao H X and Wang S G 2012 *Chin. Phys. B* **21** 110506
[22] Sun W, Chen Z and Kang Y H 2012 *Chin. Phys. B* **21** 010504
[23] Gao J X, Buldyrev S V, Stanley H E and Havlin S 2012 *Nature Phys.* **8** 40
[24] Provata A and Beck C 2012 *Phys. Rev. E* **286** 046101
[25] Zhang J and Small M 2006 *Phys. Rev. Lett.* **96** 238701
[26] Zhang J, Sun J, Luo X, Zhang K, Nakamura T and Small M 2008 *Physica D* **237** 2856
[27] Yang Y and Yang H J 2008 *Physica A* **387** 1381
[28] Lacasa L, Luque B, Ballesteros F, Luque J and Nuno J C 2008 *Proc. Natl. Acad. Sci. USA* **105** 4972
[29] Luque B, Lacasa L, Ballesteros F and Luque J 2009 *Phys. Rev. E* **80** 046103
[30] Lacasa L and Toral R 2010 *Phys. Rev. E* **82** 036120
[31] Luque B, Lacasa L, Ballesteros F J and Robledo A 2011 *PLoS One* **6** e22411
[32] Liu C, Zhou W X and Yuan W K 2010 *Physica A* **389** 2675
[33] Dong Z and Li X 2010 *Acta Phys. Sin.* **59** 1600 (in Chinese)
[34] Li P and Wang B H 2007 *Physica A* **378** 519
[35] Shirazi A H, Jafari G R, Davoudi J, Peinke J, Tabar M R R and Sahimi M 2009 *J. Stat. Mech.* P07046
[36] Campanharo A S L O, Sirer M I, Malmgren R D, Ramos F M and Amaral L A N 2011 *PLoS One* **6** e23378
[37] Xu X, Zhang J and Small M 2008 *Proc. Natl. Acad. Sci. USA* **105** 19601
[38] Marwan N, Donges J F, Zou Y, Donner R V and Kurths J 2009 *Phys. Lett. A* **373** 4246
[39] Donner R V, Zou Y, Donges J F, Marwan N and Kurths J 2010 *New J. Phys.* **12** 033025
[40] Gao Z K and Jin N D 2009 *Chaos* **19** 033137
[41] Strorzzi F, Poljansek K, Bono F, Gutierrez E and Zaldivar J M 2011 *Int. J. Bifur. Chaos* **21** 1047
[42] Donges J F, Heitzig J, Donner R V and Kurths J 2012 *Phys. Rev. E* **85** 046105
[43] Xiang R, Zhang J, Xu X K and Small M 2012 *Chaos* **22** 013107
[44] Zou Y, Donner R V, Wickramasinghe M, Kiss I Z, Small M and Kurths J 2012 *Chaos* **22** 033130
[45] Shimada Y, Ikeguchi T and Shigehara T 2012 *Phys. Rev. Lett.* **109** 158701
[46] Wang W X, Yang R, Lai Y C, Kovanis V and Grebogi C 2011 *Phys. Rev. Lett.* **106** 154101
[47] Wang W X, Yang R, Lai Y C, Kovanis V and Harrison M A F 2011 *Europhys. Lett.* **94** 48006
[48] Su R Q, Wang W X and Lai Y C 2012 *Phys. Rev. E* **85** 065201
[49] Donges J F, Zou Y, Marwan N and Kurths J 2009 *Europhys. Lett.* **87** 48007
[50] Zhou L, Gong Z Q, Zhi R and Feng G L 2009 *Acta Phys. Sin.* **58** 7351 (in Chinese)
[51] Gong Z Q, Wang X J, Zhi R and Feng A X 2011 *Chin. Phys. B* **20** 079201
[52] Song D M, Jiang Z Q and Zhou W X 2009 *Physica A* **388** 2450
[53] Qian M C, Jiang Z Q and Zhou W X 2010 *J. Phys. A: Math. Theor.* **43** 335002
[54] Zhang J, Zhang K, Feng J and Small M 2010 *PLoS Comput. Biol.* **6** e1001033
[55] Chavez M, Valencia M, Navarro V, Latora V and Martinerie J 2010 *Phys. Rev. Lett.* **104** 118701
[56] Li X and Dong Z 2011 *Phys. Rev. E* **84** 062901
[57] Hempel S, Koseska A, Kurths J and Nikoloski Z 2011 *Phys. Rev. Lett.* **107** 054101
[58] Gao Z K, Jin N D, Wang W X and Lai Y C 2010 *Phys. Rev. E* **82** 016210
[59] Gao Z K and Jin N D 2011 *Chem. Eng. Sci.* **66** 2660
[60] Gao Z K, Jin N D, Yang D, Zhai L S and Du M 2012 *Acta Phys. Sin.* **61** 120510 (in Chinese)
[61] Gao Z K and Jin N D 2012 *Nonlinear Analysis-Real World Applications* **13** 947
[62] Walker D M and Tordesillas A 2012 *Phys. Rev. E* **85** 011304
[63] Ghaffari H O and Young R P 2012 *Europhys. Lett.* **98** 48003
[64] Yook S H, Jeong H, Barabasi A L and Tu Y 2001 *Phys. Rev. Lett.* **86** 5835
[65] Zheng D F, Trimper S, Zheng B and Hui P M 2003 *Phys. Rev. E* **67** 040102
[66] Kamada T and Kawai S 1989 *Inf. Process. Lett.* **31** 7